Digital Twin of a Field Operated Grid Forming (GFM) Inverter

Renuka Loka, Mahmoud Kabalan, Thomas Holliday,
Mohanad Elsayed, Mohamed M. Zakaria Moustafa
Center for Microgrid Research,
University of St. Thomas,
St. Paul, MN 55105,
loka3402@stthomas.edu, mahmoud.kabalan@stthomas.edu, holl7906@stthomas.edu,
elsa8648@stthomas.edu, mohamed.moustafa@stthomas.edu

Thomas Bozada
U.S. Army Engineer,
Research and Development Center
Champaign, IL, USA

***Abstract*—Available grid-forming (GFM) inverter models do not sufficiently match their frequency and voltage dynamics with field-operated industry grade inverters. To overcome this, a two-fold approach is proposed that leverages field data to develop a digital twin (DT) of Grey-box inverters. Firstly, a data-driven modeling approach for the rate of change of frequency (RoCoF) is introduced to model the frequency dynamics with virtual inertia (VI). Secondly, an automated parameter update process for voltage response alignment is proposed. The DT model is developed using field data from an industry grade GFM inverter operational in a microgrid (MG). The proposed approach is validated using multiple cases by comparing the simulation response with experimental data. It was confirmed from the analysis that practical GFM inverter dynamics with unknown VI information are captured effectively by the DT model.**

***Index Terms*—Digital Twin, Grid-forming Inverters, Microgrids, Virtual Inertia, Data-driven Models**

I. Introduction

The utilization of grid-forming (GFM) inverters in the grid and microgrids (MGs) is rapidly increasing as the demand for renewable power generation has grown. The increased reliability provided by inverters is another factor in their growing dominance [1]. However, inverters lack the dynamic performance of synchronous machines (SMs), which are based on physically rotating masses. Typically, the mass of the dynamic components in SMs intrinsically gives SMs electromechanical inertia. Inertia has a direct effect on the response of SMs. The same cannot be said for inverters, which can effectively have instantaneous response times. Thus, in dynamic states, an inverter's frequency may deviate from its nominal operating point faster than SMs [2].

Industry grade GFM inverters in MGs most often utilize droop control for primary voltage and frequency regulation, with some also integrating virtual inertia (VI) to emulate SM dynamics [3]. Relying solely on droop control causes sudden frequency transients and a high rate of change of frequency (RoCoF). Including VI control improves the transient dynamics of the frequency response [4]. However, modeling VI within GFM controls to replicate industry-grade inverters is challenging. VI varies with time, and data-driven techniques have been proposed in which the state equations were linearized to capture this time-varying behavior. [5]. Linearized models are only locally valid, and large shifts in the operating point require continuous model updates. Transfer-function-based VI models using quasi-resonant controllers with varied time constants influence the time-domain frequency deviations, which are modeled as fast transients [6]. Nevertheless, these models cannot capture the slow transient dynamics of commercial inverters.

Unlike frequency, voltage response is influenced by reactive power droop slope and inner control loop dynamics. Most commercial GFM inverter vendors do not specify these control loop parameters to protect intellectual property and proprietary information, resulting in multiple unknown parameters. Electromagnetic transient modeling (EMT) is often required for detailed higher order voltage-frequency ($V - f$) controls, and to capture intermediate responses [7]. Existing literature focuses on data-driven models, which are validated using other simulation model's responses [8], [9]. Few studies present models that can adapt to various operating points of field-operated Grey-box GFM inverters with unknown VI and control loop information. A historical data model or a continuous data exchange from the GFM to the virtual model is the key component in developing reliable models, which can be achieved through the use of digital twin (DT).

DT is defined in many ways based on architecture, application, and level of model maturity. DTs are virtual images or replicas of physical systems that can continuously adapt in time as a dynamic mirror [10]. Recently, a DT model was developed for the islanded operation of a Diesel generator [11]. Despite the rapid development of MG and the growing interest in using DT modeling for MG applications, there are currently few real-world DT implementations that deliver tangible, data-driven value to MG operators [12]. While real-time applications for evaluating MG resilience have been explored, the inherent complexities of transient, time-domain modeling

Effort sponsored by the U.S. Government under Other Transaction for Prototype Agreement number W9132T239C007 between UNIVERSITY OF ST. THOMAS and the Government. The U.S. Government is authorized to reproduce and distribute reprints for Governmental purposes not withstanding any copyright notation thereon.

The views and conclusions contained herein are those of the authors and should not be interpreted as necessarily representing the official policies or endorsements, either expressed or implied, of the U.S. Government.

This project was made possible in whole or in part by a grant from the Minnesota Department of Commerce through the Minnesota Renewable Development Account, which is financed by Xcel Energy ratepayers.

979-8-3315-8138-1

at device-level for GFM inverters continue to pose significant challenges [13]. To bridge the modeling gap between field-operated GFM inverters and simulation models, this paper presents a DT model using data-driven approach for RoCoF estimation combined with adaptive parameters within the EMT modeling of GFM inverters. The contributions are as follows:

- Introducing a data-driven VI estimation algorithm coordinated within the model-based approach.
- Developing a DT model of an industry-grade 125 kVA inverter operated within the CMR microgrid.
- Validation of the proposed method is performed using field data acquired at a high sampling rate in accordance with the IEEE 1547 standard, utilizing a GFM inverter to evaluate the effectiveness of the DT model.

II. Adaptive GFM Inverter Model

An industry grade MG installation at the center for Microgrid Research (CMR) is utilized for the proposed DT model and validation [14]. Experimental set-up at CMR is depicted in Fig. 1. The commercial Grey-box GFM inverter rated at 125 $kW/kVAR$ is driven by a 396 kWh ESS. Inverter and load bank are connected to the MG bus using independent circuit breakers (CB_{ess}, CB_{load}). A Beckhoff data acquisition (DAQ) system and SEL 451 relays are connected to the measurement transformers. Breakers can be controlled using the MG controller's (RTAC 3555) accessed though a human machine interface (HMI) using the MG network on an engineering workstation. Modbus TCP is used to communicate data between MG controller and relays.

The GFM inverter model developed for simulating commercial Grey-box inverters is depicted in Fig. 2. These inverters have inherent non-linear characteristics, ramp-rate constraints, unknown parameters, and limited inner control loop information for modeling droop settings. Traditional techniques cannot account for these varied dynamics and missing data. To overcome these issues, adaptive droop and voltage regulation combined with data-driven RoCoF modeling are proposed to develop field-validated models. The instantaneous active and

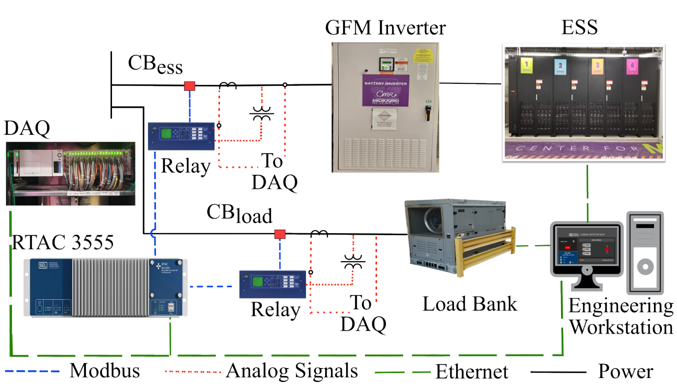

Fig. 1. Experimental set up at the Center for Microgrid Research for filed-data collection from grid forming inverters under various operational scenarios.

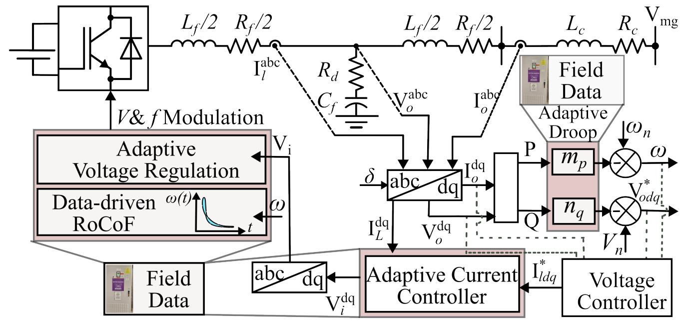

Fig. 2. Schematic of grid-forming inverter with data-driven modeling included in the traditional droop-based control loops.

reactive power are calculated based on the feedback voltage and frequency as shown in Fig. 2,

$$\begin{aligned} \tilde{p} &= v_{od} i_{od} + v_{oq} i_{oq}, \\ \tilde{q} &= v_{od} i_{oq} - v_{oq} i_{od} \end{aligned} \tag{1}$$

where V_{od}, and V_{oq} are the dq reference voltage, while the currents correspond to i_{od}, and i_{oq}. The instances of active and reactive power pass through low-pass filters with cut of frequency ω_c to obtain fundamental active and reactive power components.

$$\begin{aligned} P &= \frac{\omega_c}{s + \omega_c} \tilde{p}, \\ Q &= \frac{\omega_c}{s + \omega_c} \tilde{q} \end{aligned} \tag{2}$$

The droop controller is utilized to regulate the active and reactive power output of the GFM inverter when the system load varies and is modeled as [3],

$$\begin{aligned} \omega &= \omega_n - m_p \cdot T_F \cdot P, \\ V_{od}^* &= V_n - n_q \cdot T_F \cdot Q, and \\ V_{oq}^* &= 0, \end{aligned} \tag{3}$$

where P and Q are fundamental active and reactive power components, ω_n is the nominal angular frequency in rad/s, V_n is the nominal system voltage, and T_F is the low pass filter transfer function. where m_p and n_q are adaptive real and reactive power droop coefficients, varied within the limits $m_{pmin} \leq m_p \leq m_{pmax}$ and $n_{qmin} \leq n_q \leq n_{qmax}$ to match the steady state operation observed in the field data and calculated using the following equations:

$$\begin{aligned} m_P &= \frac{w_{max} - w_{min}}{P_{max}} \\ n_q &= \frac{V_{max} - V_{min}}{Q_{max}} \end{aligned} \tag{4}$$

where $P_{\max}$ represents the nominal real power of the inverter, and $\omega_{\max}$ and $\omega_{\min}$ denote the maximum and minimum operating frequencies determined by the specified droop percentage. Similarly, $Q_{\max}$ corresponds to the nominal reactive power of the inverter, while $V_{\max}$ and $V_{\min}$ represent the maximum and minimum voltage limits defined by the voltage droop settings.

979-8-3315-8138-1

The output from droop regulation is sent to the voltage controller, which provides a reference, i^*_{ldq}, for the current controller, which is modeled as:

$$\begin{aligned} v^*_{id} &= -\sigma_{dc}\omega_n L_f i_{lq} + K_{pc}(i^*_{ld} - i_{ld}) + K_{ic}\gamma_d, \\ v^*_{iq} &= \sigma_{qc}\omega_n L_f i_{ld} + K_{pc}(i^*_{lq} - i_{lq}) + K_{ic}\gamma_q \end{aligned} \tag{5}$$

where $\gamma_d = \int(i^*_{ld} - i_{ld})$ and $\gamma_q = \int(i^*_{lq} - i_{lq}).K_{pc}$ and K_{ic} are the proportional-integral (PI) controller gains. Current entering the filter after transformation to dq-reference frame is i_{ldq} and reference from voltage controller is i^*_{ldq}. The gains, σ_{dc} and σ_{qc} are designed to be adaptive by using field data to minimize the error between measured and simulated step response. The adaptive voltage regulation loop is modeled using adjustable gains and ramp-rate using the below equation:

$$\frac{dV_i}{dt} = \begin{cases} R_\mathrm{r}, & \text{if } V_\mathrm{i}(t) - V_\mathrm{i}^*(t) > R_\mathrm{r} \cdot \Delta t \\ -R_\mathrm{f}, & \text{if } V_\mathrm{i}(t) - V_\mathrm{i}^*(t) < -R_\mathrm{f} \cdot \Delta t \\ \frac{V_\mathrm{i}^*(t) - V_\mathrm{i}(t)}{\Delta t}, & \text{otherwise} \end{cases} \tag{6}$$

where R_r and R_f are adjustable ramp rates for the output V_i from the current controller, which is modulated using V_i^*, within the simulation interval Δt. For modeling the nonlinear frequency ramping characteristics due to VI, data-driven estimation model for RoCoF is introduced in the GFM inverter control loops using

$$RoCoF = \dot{\omega}(t) = f'(\omega(t), u(t)) \tag{7}$$

where $f(\omega(t))$ is a nonlinear function obtained using data-driven modeling for an input $u(t)$. To enable continuous model updates within the data-driven framework, the development of the DT model is presented in the subsequent section.

III. Digital Twin Model

In developing a DT for GFM inverters, it is essential to establish a framework capable of ensuring alignment between the virtual model and the physical inverter. Accordingly, DT model synchronizes its operation using information from the field-operated GFM inverters. Experimental data is archived in a database, enabling continuous updates of operation set -points in the virtual model. Fig. 3 illustrates the end-to-end process of DT model development, showing data-driven updates within the EMT model and synchronization with the physical inverter set-up. The point-on-wave frequency response data from the database is processed using MATLAB to provide fitted RoCoF curve, obtained as nonlinear time dependent functions using polynomial regression:

$$f(\omega(t), u(t)) = a_4 t^4 + a_3 t^3 + a_2 t^2 + a_1 t + a_0 \tag{8}$$

where a_0, a_1, a_2, a_3, a_4 are the polynomial coefficients obtained from fitting the point-on-wave frequency response data. These coefficients capture the nonlinear, time-dependent behavior of the RoCoF response and are determined for each operating condition of the GFM inverter. Using (7), data-driven RoCoF model is estimated and deviations in the time-dependent curve at vaious sampling instants are represented

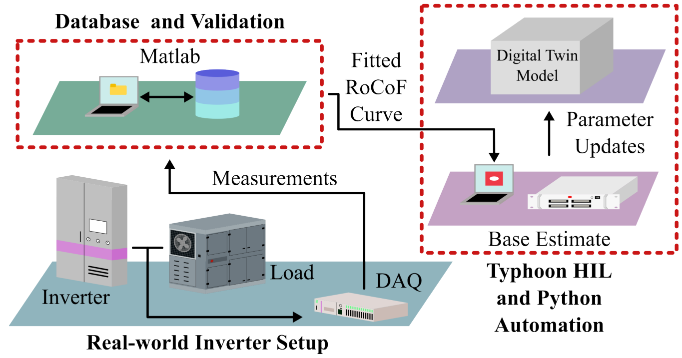

Fig. 3. Line diagram illustrating the grid-forming inverter digital twin development process.

using multipart functions. By rearranging (7) as discrete multipart functions, the estimated RoCoF for EMT model updates is given as:

$$RoCoF = \dot{\omega}(t) = \sum_{i=1}^{n} f_i'(\omega(t), u(t)) \tag{9}$$

Experimental results from the inverter under different loading scenarios are then used to continuously update the RoCoF curve of the simulated model.

For voltage response alignment, the set of adaptive parameters from control loop equations (3) - (6) of the GFM inverter are first defined as

$$\theta = \begin{bmatrix} m_p & n_q & \sigma_{dqc} & R_r & R_f \end{bmatrix}, \tag{10}$$

which are iteratively tuned to minimize the error, modeled as:

$$\begin{aligned} \min_{\theta} \quad & \delta(\theta) = \frac{1}{N}\sum_{k=1}^{N} \left\| \mathcal{X}^{V,f}(t_k) - \rho^{V,f}(t_k) \right\|, \\ \text{s.t.} \quad & \delta(\theta) \leq \epsilon_\theta \end{aligned} \tag{11}$$

Here, $\mathcal{X}^{V,f}(t_k)$ represents the experimental voltage and frequency data obtained from step load tests on the GFM inverter, and $\rho^{V,f}(t_k)$ corresponds to the simulated voltage and frequency response. ϵ_θ denotes the maximum allowable error. The adaptive parameters are estimated using a semi-automated process that tunes step-response characteristics, including peak overshoot, transient time, and settling time.

These updated parameters, together with the data exchange from the field-operated inverter and the control loops modeled in Section II, are utilized for voltage alignment through error minimization using Python scripts. This process creates a highly accurate virtual replica of the GFM inverter, resulting in a robust DT model.

IV. Case Studies on DT Model

Data is recorded at a sampling rate of $20\,kHz$ for various step load changes of active and reactive power in accordance with IEEE 1547.1-2020 STD, section 4.6.3 and section 5 [15]. The droop settings of the commercial inverter are at

979-8-3315-8138-1

TABLE I
DATA-DRIVEN AND ADAPTIVE PARAMETERS FOR FREQUENCY REGULATION

P (kW)	a_4	a_3	a_2	a_1	m_p
0–25	1.09e-08	-1.16e-05	0.001212	-0.04486	1.92e-05
25–50	-2.00e-06	0.000455	-0.03763	1.327	1.92e-05
50–75	3.06e-07	-0.0001086	0.01455	-0.9051	1.92e-05
75–100	3.21e-06	-0.002125	0.5282	-58.41	1.80e-05
100–125	3.89e-07	-0.0004374	0.1843	-34.56	1.80e-05
	0.004178	0.009743	0.004462	-0.1377	1.79e-05

52 kW/Hz and -0.154 $V/kVAR$, which represent a 4% $V-Q$ and $P-f$ droop, and VI parameter is set to 200. DT model as detailed in Section III is developed for the field-operated GFM in CMR MG. The DT model response is captured and validated with the physical inverter response.

A. Frequency and Voltage Response

The frequency response database for the GFM is created for different operating points by varying the load in steps of 25 kW from no load to the inverter's rated load of 125 kW. Coefficients for the nonlinear function described in (8) for RoCoF estimation are obtained for different set points using bi-square polynomial regression are shown in Table. I. Using (9), the DT model's frequency response is updated in real-time using EMT simulations to replicate the trasnient dynamics. Steady state field data is used to adjust the frequency droop-coefficient, m_p.

The DT model's frequency response for various step load changes are depicted in Fig. 4. It is observed for multiple cases $((0-25\,kW), (25-50\,kW), (75-100\,kW), (100-125\,kW))$, frequency response of data-driven RoCoF estimation aligns with the field data of industrial Grey-box GFM inverter. These RoCoF variations are not instantaneous as opposed to simulations in previous studies [6], which highlights the applicability of the proposed method.

The gains influencing transient response of the voltage dynamics are σ_{dc}, R_R, R_f. Model initialization is performed with a set of $[5\ 0\ -1000]$ parameters. These are dynamically adaptive in real-time, which adjust their values automatically after the step disturbance. During $0-25\,kVAR$ step load change with constant active power, the automated parameters adjusted after a 200 ms delay are $[5\ 100\ -50]$. In another case of $25-50\,kVAR$, the adaptive parameters modified after 25 ms are $[1.33\ 200\ -40]$. All the adaptive parameters are automatically adjusted according to the load disturbance by leveraging python based real-time automation scripts executed in Typhoon HIL SCADA environment. The voltage response for the corresponding reactive power load change cases is depicted in Fig. 5. Transient response of the voltage deviation aligns with the field data with slight variations in the rise time and peak overshoot whereas the steady state aligns with greater accuracy. The results demonstrate settling-time alignment in the voltage deviation.

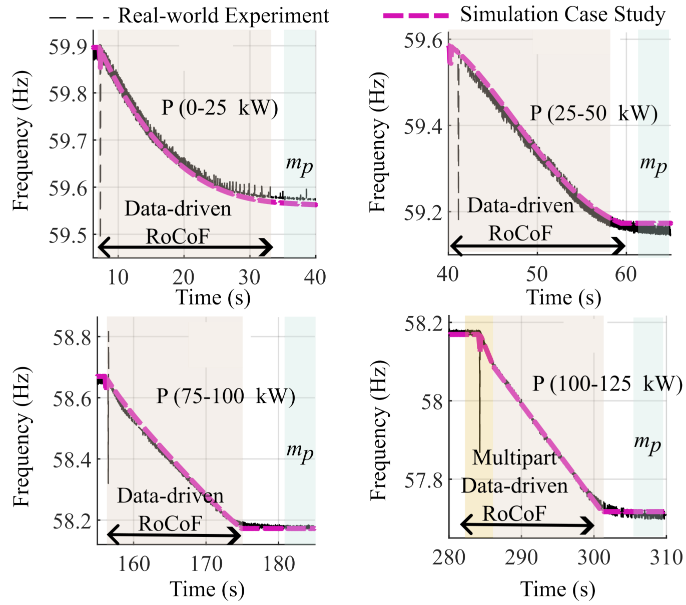

Fig. 4. Comparison of time domain response of frequency dynamics using real-time data-driven nonlinear function implementation for RoCoF modeling.

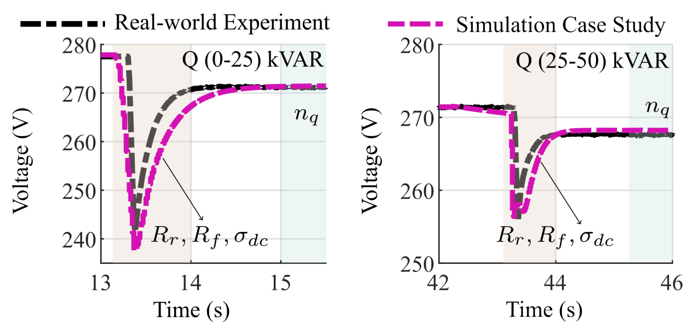

Fig. 5. Comparative time domain response of voltage deviation while implementing real-time adaptive inner control loops.

B. Performance Analysis

The time domain frequency response of the simulation case studies closely aligns with the results captured in the real world experiments as shown in Fig. 4. In Fig. 6, per unit error between the simulation response and their corresponding real-world experiments is visualized for real-power deviations. At steady state, the frequency deviation is minimal, with the $75-100\,kW$ case exhibiting an accuracy of 99.96%. This indicates a maximum error of 0.004 pu deviation from the steady-stae response of the field operated inverter. During transients, the minimum recorded accuracy is 99.4% in the $0-25\,kW$ transition, with a maximum error 0.6%, indicated the robust performance of DT model in capturing the physical inverter's dynamics.

The voltage response of the virtual model is less accurate than the frequency response. This is mainly due to the real-world GFM inverter having faster voltage rise times than the virtual model. In both cases shown in Fig. 7, there is an initial increase in the error as soon as the load increases.

979-8-3315-8138-1

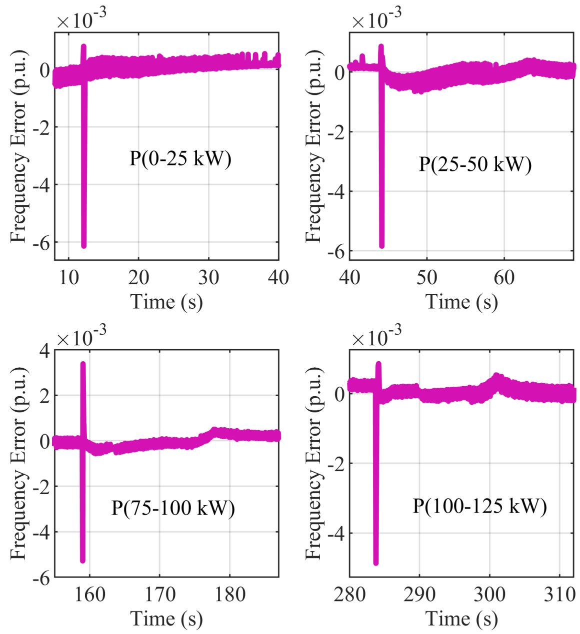

Fig. 6. Per unit error in frequency between the time domain of frequency dynamics in the real-world experimental results and simulation case study.

Since the real-world GFM's voltage decreases faster, the error between it and the virtual model increases rapidly. However, the alignment and similarity of the peak overshoots causes a sharp decrease in the error once the peak values are reached. Once again, the error increases immediately after the peak values are reached, as the real-world GFM is able to increase its voltage faster than the virtual model. The difference in voltage response times results in a minimum 92.4% accuracy for the virtual model during transients and a steady state accuracy of 99.8%.

V. Conclusion

Modeling the dynamics of Grey-box inverters is challenging due to limited control loop information and nonlinear characteristics of VI. An adaptive data-driven technique for RoCoF is developed for frequency response modeling. In addition, inner control loop parameter estimation model has been implemented to represent voltage deviations. These parameters are triggered in real-time to replicate the practical behavior of the commercial GFM inverters operational in MG, resulting in a highly accurate DT model. Validation of multiple step response cases using high resolution field data demonstrated that the proposed method efficiently follows the RoCoF response, confirming the applicability of the model for capturing reliable device level dynamics. The voltage response follows the experimental results with slight transient deviation, which can be investigated in future studies. In conclusion, VI in GFM inverters introduces a nonlinear RoCoF response that is specific to each load disturbance. The proposed method captures this behavior regardless of the actual VI setting, confirming its suitability for modeling industrial inverters with unknown parameters.

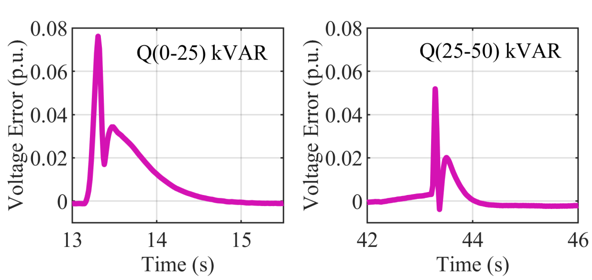

Fig. 7. Per unit error in voltage between the time domain of frequency dynamics in the real-world experimental results and simulation case study.

References

[1] K. Y. Yap, C. R. Sarimuthu, and J. M.-Y. Lim, "Virtual inertia-based inverters for mitigating frequency instability in grid-connected renewable energy system: A review," *Applied Sciences*, vol. 9, no. 24, 2019.

[2] E. Rakhshani and P. Rodriguez, "Inertia emulation in ac/dc interconnected power systems using derivative technique considering frequency measurement effects," *IEEE Transactions on Power Systems*, vol. 32, no. 5, pp. 3338–3351, 2017.

[3] X. Lyu, W. Du, S. M. Mohiuddin, and Y. Cheng, "Critical clearing time for droop-controlled grid-forming inverters with circular current limiting and virtual impedance current limiting," vol. 40, no. 2, pp. 1997–2000.

[4] B. She, F. Li, J. Wang, H. Cui, X. Wang, and R. Bo, "Virtual inertia scheduling (VIS) for microgrids with static and dynamic security constraints," vol. 16, no. 2, pp. 785–796.

[5] B. Tan and J. Zhao, "Data-driven time-varying inertia estimation of inverter-based resources," vol. 38, no. 2, pp. 1795–1798.

[6] S. Luo, W. Chen, X. Li, and Z. Hao, "A new virtual inertial strategy for andronov–hopf oscillator based grid-forming inverters," vol. 12, no. 2, pp. 1995–2005.

[7] S. Helman, H. Jung, N. Baeckeland, D. Ramasubramanian, and S. Dhople, "Grey-box system identification of grid-forming inverters," in *2024 9th IEEE Workshop on the Electronic Grid (eGRID)*, pp. 1–6, IEEE.

[8] N. Guruwacharya, S. Chakraborty, G. Saraswat, R. Bryce, T. M. Hansen, and R. Tonkoski, "Data-driven modeling of grid-forming inverter dynamics using power hardware-in-the-loop experimentation," *IEEE Access*, vol. 12, pp. 52267–52281, 2024.

[9] S. Helman, H. Jung, N. Baeckeland, D. Ramasubramanian, and S. Dhople, "Grey-box system identification of grid-forming inverters," in *2024 9th IEEE Workshop on the Electronic Grid (eGRID)*, pp. 1–6, 2024.

[10] C. Brosinsky, X. Song, and D. Westermann, "Digital twin - concept of a continuously adaptive power system mirror," in *International ETG-Congress 2019; ETG Symposium*, pp. 1–6, 2019.

[11] R. Loka, M. Kabalan, T. Holliday, and T. Bozada, "Digital twin model of an islanded diesel generator," in *2025 IEEE Power Energy Society General Meeting (PESGM)*, pp. 1–5, 2025.

[12] N. Bazmohammadi, A. Madary, J. C. Vasquez, H. B. Mohammadi, B. Khan, Y. Wu, and J. M. Guerrero, "Microgrid digital twins: Concepts, applications, and future trends," *IEEE Access*, vol. 10, pp. 2284–2302, 2022.

[13] M. R. Jamieson, Q. Hong, J. Han, S. Paladhi, and C. Booth, "Digital twin-based real-time assessment of resilience in microgrids," in *11th International Conference on Renewable Power Generation-Meeting net zero carbon (RPG 2022)*, vol. 2022, pp. 213–217, IET, 2022.

[14] M. Kabalan, I. Masui, and H. Gamit, "Design, testing, and implementation of a microgrid controller using iec 61131-3," in *2022 IEEE Power Energy Society General Meeting (PESGM)*, pp. 1–5, 2022.

[15] "Ieee standard conformance test procedures for equipment interconnecting distributed energy resources with electric power systems and associated interfaces," *IEEE Std 1547.1-2020*, pp. 1–282, 2020.

979-8-3315-8138-1